Measurement of Individual Red Blood Cell Motions Under High Hematocrit Conditions Using a Confocal Micro-PTV System

Rui Lima,[1,2,3] Takuji Ishikawa,[1] Yohsuke Imai,[1] Motohiro Takeda,[1,4] Shigeo Wada,[5] and Takami Yamaguchi[6]

[1]Department of Bioengineering and Robotics, Graduate School of Engineering, Tohoku University, 6-6-01 Aoba, Sendai 980-8579, Japan; [2]Department of Mechanical Technology, ESTiG, Braganca Polytechnic, C. Sta. Apolonia, 5301-857 Braganca, Portugal; [3]CEFT, Faculdade de Engenharia da Universidade do Porto, Rua Dr. Roberto Frias, 4200-465 Porto, Portugal; [4]Division of Surgical Oncology, Graduate School of Medicine, Tohoku University, 2-1 Seiryo-machi, Aoba-ku, Sendai 980-8575, Japan; [5]Department of Mechanical Science and Bioengineering, Graduate School of Engineering Science, Osaka University, Toyonaka, Osaka 560-8531, Japan; and [6]Department of Biomedical Engineering, Graduate Biomedical School of Engineering, Tohoku University, 6-6-01 Aoba, Sendai 980-8579, Japan

Abstract—Developments in optical experimental techniques have helped in elucidating how blood flows through microvessels. Although initial developments were encouraging, studies on the flow properties of blood in microcirculation have been limited by several technical factors, such as poor spatial resolution and difficulty obtaining quantitative detailed measurements at such small scales. Recent advances in computing, microscopy, and digital image processing techniques have made it possible to combine a particle tracking velocimetry (PTV) system with a confocal microscope. We document the development of a confocal micro-PTV measurement system for capturing the dynamic flow behavior of red blood cells (RBCs) in concentrated suspensions. Measurements were performed at several depths through 100-μm glass capillaries. The confocal micro-PTV system was able to detect both translational and rotational motions of individual RBCs flowing in concentrated suspensions. Our results provide evidence that RBCs in dilute suspensions (3% hematocrit) tended to follow approximately linear trajectories, whereas RBCs in concentrated suspensions (20% hematocrit) exhibited transversal displacements of about 2% from the original path. Direct and quantitative measurements indicated that the plasma layer appeared to enhance the fluctuations in RBC trajectories owing to decreased obstruction in transversal movements caused by other RBCs. Using optical sectioning and subsequent image contrast and resolution enhancement, the system provides previously unobtainable information on the motion of RBCs, including the trajectories of two or more RBCs interacting in the same focal plane and RBC dispersion coefficients in different focal planes.

Keywords—Blood flow, Microcirculation, Red blood cells, Confocal micro-PTV, RBC dispersion, Microchannels.

Address correspondence to Rui Lima, Department of Bioengineering and Robotics, Graduate School of Engineering, Tohoku University, 6-6-01 Aoba, Sendai 980-8579, Japan. Electronic mail: rui@pfsl.mech.tohoku.ac.jp

INTRODUCTION

Blood flow in the microcirculation depends on several combined effects, including cell deformability, flow shear rates, and vessel wall deformability, as well as biochemical and physiological factors. One of the first observations of the non-Newtonian behavior of blood flowing in capillaries was achieved by Fahraeus and Lindqvist,[7] who found that the apparent viscosity decreases with microtube diameter, in contrast to Poiseuille's law, for capillaries less than 300 μm in diameter. However, explanations for this finding were only provided in the 1970s through microscopic observations.[5,8,11,12,30] The most plausible explanation relies on the formation of a cell-free plasma layer near the wall, with red blood cells (RBCs) tending to migrate toward the center of the microtube. Extensive research ensued on the flow properties of blood in both dilute and concentrated suspensions using several measuring techniques such as double-slit photometry,[2,10] video microscopy and image analysis,[8,11,12,29] laser-Doppler anemometry,[3,35] and particle-measuring methods.[20,21,32,36] Although extensive studies have been conducted on the microhemodynamic behavior of single RBCs in dilute suspensions, their behavior in concentrated suspensions remains poorly understood, in part due to technical limitations. The main limitation in measuring high concentrations is the attenuation of incident light owing to hemoglobin absorption and light scattering by the RBCs themselves. Thus, despite recent advances in microscopy, blood flow phenomena at a microscopic level, particularly in concentrated suspensions, remain unclear.

Results from Goldsmith and his colleagues (see Goldsmith *et al.*[14] for review) regarding the flow

behavior of RBCs in glass capillaries have provided the most insight into several microrheological phenomena occurring in highly concentrated RBC suspensions. However, their research employed transparent ghost cell suspensions to avoid light absorption by hemoglobin, which strongly influences the mechanical properties of RBC membranes. By removing hemoglobin, the membrane mechanical properties might have been altered appreciably, consequently changing the rheological behavior.[4,13,27,31] In addition, conventional microscopy illuminates the entire flow region, providing high background noise from out-of-focus emitted light and thereby degrading flow measurements.[6,25] Hence, more accurate measurements in concentrated RBC suspensions are required to gain further insight into complex microhemodynamic phenomena.

Recent progress in confocal microscopy[6,15] have led to a new technique known as confocal microparticle image velocimetry (PIV).[17,20–22,28,33] This method combines conventional PIV with a spinning disk confocal microscope (SDCM) to obtain in-focus images with an optical thickness of less than 1 μm (optical sectioning effect). The superior spatial resolution and improved contrast and definition allow the measurement of several microrheology phenomena in concentrated suspensions of RBCs. Recently, our confocal system was combined with a cross-correlation technique to obtain detailed information on the *in vitro* velocity profiles of blood with hematocrits (Hcts) up to 17%.[20] However, velocity field errors resulting from trace particles necessitate combining the developed confocal system with a single particle tracking (SPT) method to characterize higher Hct level phenomena. To our knowledge, this study provides the first confocal microparticle tracking velocimetry (PTV) measurements for studying microrheology in highly concentrated erythrocyte suspensions.

This study demonstrates the ability of our confocal micro-PTV system to obtain detailed qualitative and quantitative information on the behavior of individual RBCs flowing through 100-μm glass capillaries. Measurements were performed at 20 μm from the bottom wall (20% Hct; Reynolds number (Re), ~0.006). We also measured radial displacement and dispersion coefficients at several depths and Hcts (3, 15, and 35%).

MATERIALS AND METHODS

Blood Cell Labeling

We examined four working fluids: Dextran 40 (Dx-40; Otsuka Medicine, Tokyo, Japan) containing 3% (3% Hct), 15% (15% Hct), or 35% (35% Hct) human RBCs, and Dx-40 containing 20% (20% Hct) RBCs and 2% white blood cells (WBCs). Both the RBCs and WBCs were labeled with a lipophilic carbocyanime derivative, chloromethylbenzamido (CM-Dil, C-7000, Molecular Probes, Eugene, OR, USA). This cell tracker was selected because of its strong photostable fluorescence, excellent cellular retention, and minimal cytotoxicity (see Fig. 1).

Blood was collected from a healthy adult volunteer (age, 33 years); ethylenediaminetetraacetic acid (EDTA) was used to prevent coagulation. RBCs were separated by centrifugation (1500 rpm, 20 min), and the plasma and buffy coat were removed by aspiration; washing and centrifugation with physiological saline (PS) were repeated twice. The washed RBCs were diluted with PS to make several samples with hematocrit levels of ~40% by volume. All blood samples were stored hermetically at 4 °C until labeling.
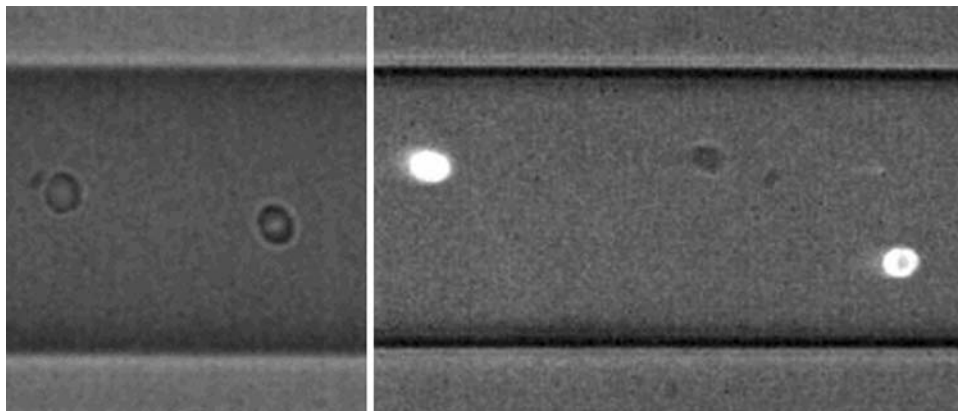

FIGURE 1. Halogen and confocal images of fluorescently labeled RBCs. The blood cells were labeled with a lipophilic carbocyanime derivative, chloromethylbenzamido (CM-Dil, C-7000). On the left side two RBCs appear as bright spots from laser-emitted light.

The procedure for labeling both RBCs and WBCs was as follows:

1. Centrifuge the blood sample (1 mL with 40% Hct) at 2000 rpm for 5 min;
2. Remove all PS and add 200 μL of fresh PS and 10 μL of cell tracker CM-Dil, C-7000 (50 μg, diluted with 200 μL of ethanol);
3. Mix gently and incubate for 30 min at 37 °C, and then for 1–2 h at 4 °C;
4. Add approximately 500 μL of PS and mix gently;
5. Centrifuge the solution (2000 rpm, 5 min) and remove the excess dye; and
6. Resuspend the washed cells in Dx-40 to the required RBC or WBC concentration by volume.

Owing to possible loss of blood cells during labeling, the Hct of each sample was measured using a Hct centrifuge (Kubota 3220; Kubota Corp., Osaka, Japan) prior to the experiment. Note that WBCs were obtained using a lymphoprep tube (Axis-Shield, Oslo, Norway) according to the separation procedure recommended by the manufacturer. Using this approach, fluorescently labeled RBCs comprised about 10% of the total cell volume (40% Hct).

All procedures were carried out in compliance with the guidelines of the Ethics Committee on Clinical Investigation of Tohoku University.

Glass Microchannels

A 100-μm, circular, borosilicate glass microchannel was fabricated by Vitrocom (Mountain Lakes, NJ, USA). The microchannel was mounted on a slide glass approximately 80 μm thick and immersed in glycerol of the same refractive index to minimize refraction from the walls.

Experimental Setup

The confocal micro-PTV system consisted of an inverted microscope (IX71; Olympus, Tokyo, Japan) combined with a confocal scanning unit (CSU22; Yokogawa, Tokyo, Japan) and a diode-pumped solid state (DPSS) laser (Laser Quantum Ltd., Stockport, UK), using an excitation wavelength of 532 nm. A high-speed camera (Phantom v7.1; Vision Research, NJ, USA) was connected to the outlet port of the CSU22 (Fig. 2). The glass microtube was placed on the stage of the inverted microscope, where the flow rate of the working fluids was kept constant using a syringe pump (KD Scientific Inc., Holliston, MA, USA). The Re and associated experimental parameters are summarized in Table 1. Using a thermo-plate controller (Tokai Hit, Shizuoka, Japan), the temperature around the microtube was maintained at 36 ± 1 °C.

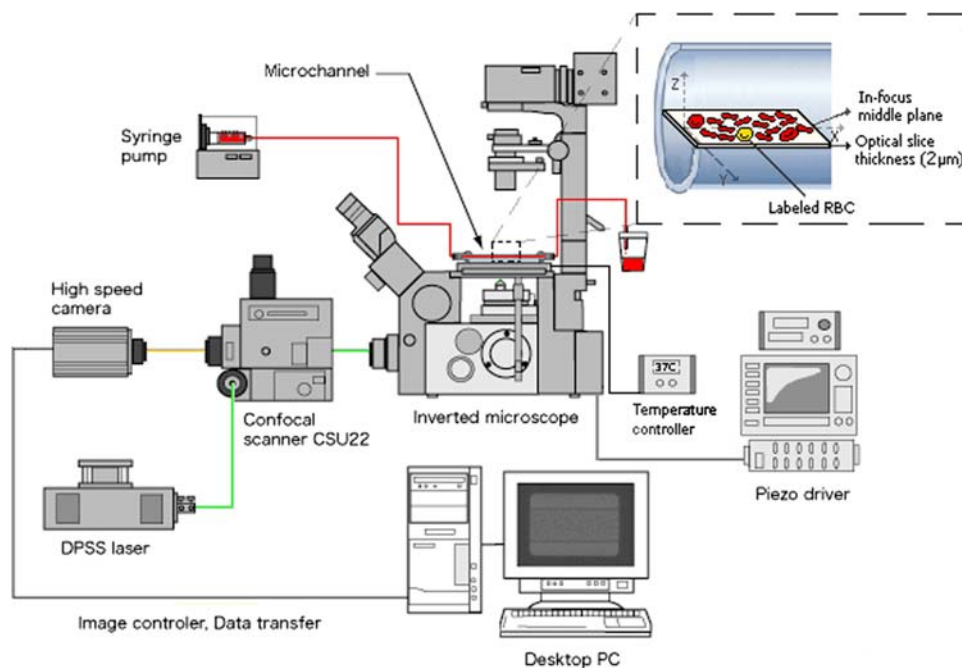The laser illuminated the glass microchannel from beneath the microscope stage, through a dry ×40

FIGURE 2. Confocal micro-PTV experimental setup. The confocal system consisted of an inverted microscope combined with a confocal scanning unit (CSU22), a DPSS laser, and a high-speed camera (Phantom v7.1).

TABLE 1. Experimental parameters used to calculate the Re.

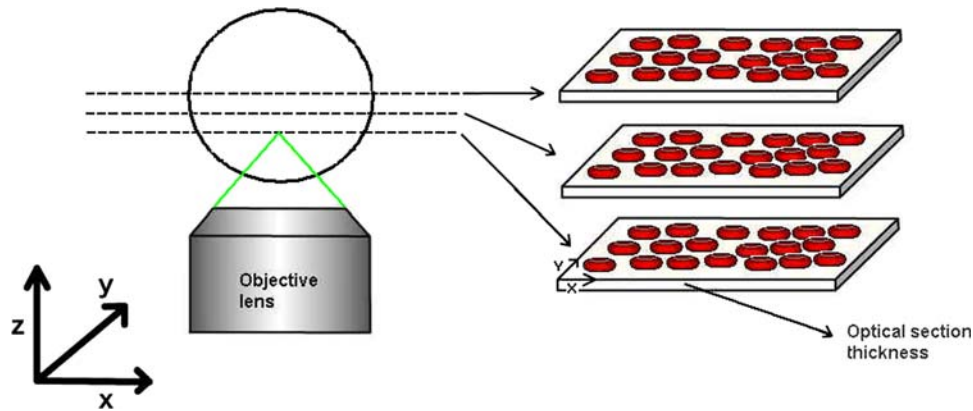| Experiment	n^a	Hct (%)	Density (kg/m^3)	Mean velocity (m/s)	Diameter (m)	Viscosity of Dx-40 (Ns/m^2)	Re
RBC and WBC flow near the wall ($z = 20$ μm)	51	20	1046	2.5×10^{-4}	10^{-4}	4.5×10^{-3}	0.0058
RBC dispersion at a series of optical sections	74	3	1046	1.63×10^{-4}	10^{-4}	4.5×10^{-3}	0.0038
	92	15	1046	1.85×10^{-4}	10^{-4}	4.5×10^{-3}	0.0043
	46	35	1046	1.8×10^{-4}	10^{-4}	4.5×10^{-3}	0.0042

^{a}Number of labeled RBCs.

FIGURE 3. Diagram showing the ability of the confocal system to generate optical sectioned images along the z-axis. The optical slice thickness (OST) was 2 μm based on geometric–optical analysis criteria.[22] Images were captured with a resolution of 640 × 480 pixels, at a rate of 100 frames/s with an exposure time of 9.4 ms. The temporal resolution of the measurements was 10 ms.

objective lens with a numerical aperture of 0.9. Satisfactory illumination of the labeled RBCs and WBCs, which absorbed green light (excitation peak, 553 nm) and emitted yellow light (emission peak, 570 nm), was achieved. The optical slice thickness was 2 μm, based on geometric-optical analysis criteria[22] (Fig. 3).

A series of xy confocal images was captured in 12-bit gray scale, with a resolution of 640 × 480 pixels, and at a rate of 100 frames/s using an exposure time of 9.4 ms, which corresponded to a temporal resolution of 10 ms. The use of this long exposure time (9.4 ms) allowed us to improve the image brightness owing to an increase in the residence time of the labeled RBCs, which enabled the gathering of sufficient photons for image formation. As a result, it was possible to track labeled RBCs from one picture to the next. Recorded images were evaluated with Image J[1] software (NIH, Bethesda, MD, USA), using the manual tracking MtrackJ[23] plug-in.

Tracking Single RBCs: Trajectory, Collision, and Rolling

Using the labeling procedure described above, most of the RBCs were uniformly labeled along the entire membrane surface (see Fig. 1). The fluorescently labeled RBCs lying in the focal plane of interest appeared as bright dots, with the highest emitted light intensity. To minimize the effects of the fainter RBCs passing through the region of interest but above and below the focal plane, a specific threshold intensity level was chosen. Thus, data for all labeled RBCs with intensities below 100 (8-bit grayscale; min–max, 0–255) were discarded. An exception was made when examining the interaction effects of WBCs on the motion of RBCs.

The RBCs were followed in flow for periods of time from 0.34 to 1 s, with a temporal resolution of 10 ms. To determine the motion of selected RBCs, they were manually tracked through successive images, using the intensity-weighted mean position of pixels above a threshold (bright centroid). With this method, it was possible to track labeled RBCs even when two cells were in close proximity. After obtaining a series of x and y positions, the data were exported for the determination of physical quantities such as the velocity, radial and transversal displacement, and dispersion coefficient, using proprietary C code software.[18]

The brightness of fluorescently labeled RBCs depended strongly on their location within the microchannel. During the experiments, especially at locations close to the bottom wall (strongest incident

light), we found that a small percentage of RBCs (less than 1% of the total cell volume) were partially labeled, creating small localized markers along the membrane. This phenomenon allowed us to determine the membrane motion of the partially labeled RBCs flowing near the microchannel wall ($z = 20\ \mu m$). Note that for this case, the tracking of the membrane motion was based on the bright centroid criteria, whereas the translational motion was based on the dark centroid criteria, using the MtrackJ[23] software.

RESULTS

To analyze the ability of the confocal micro-PTV system to track RBCs, labeled RBCs at several Hcts (3–35%) were followed. To calculate dispersion coefficients (D_{yy}), measurements were performed at a series of optical sections. For complex microrheological events in flowing blood, such as RBC interaction and orientation, all measurements were performed near the microchannel wall ($z = 20\ \mu m$) with ~20% Hct. Wall region phenomena are of primary interest due to the lack of understanding surrounding mass transport mechanisms in thrombogenesis.[26,37]

Blood Flow Visualization

RBC and WBC Flow at 20% Hct

The interactions of blood cells in flowing blood and their orientations were measured *in vitro* at 20% Hct and Re ~ 0.006. Examples of recorded images in both the center and bottom planes ($z = 20\ \mu m$) are presented (Fig. 4). In Fig. 4a, the plasma layer formed is clearly visible. In Fig. 4b, it is possible to see both labeled and unlabeled RBCs. Figures 4c and 4d are confocal images used to track blood cells. Note that in Fig. 4d, the brightness and contrast of the image were adjusted to better visualize both RBCs and WBCs. For a video of *in vitro* blood (20% Hct; Re ~ 0.006) flowing around the center plane, see Electronic supplementary material 1 online.

RBC Flow at Several Hcts Around the Middle Plane

RBCs in flowing blood exhibit a random-like, transverse motion, which is dependent on the Hct. Dispersion of labeled RBCs was measured in the center plane at several Hcts (3, 15, 35%) at a Re of ~0.004. Figure 5 shows images recorded with both labeled and unlabeled RBCs at several Hcts. It is evident that
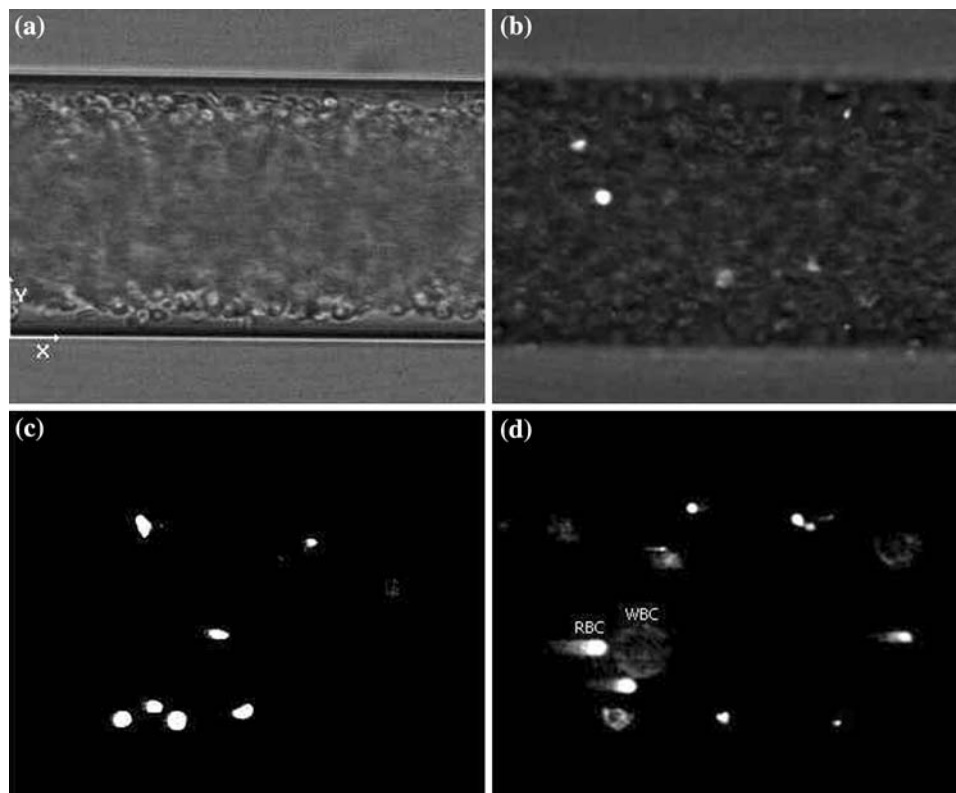

FIGURE 4. (a) An image of the blood used in this experiment with halogen illumination recorded in the center plane. (b) An image with labeled RBCs (bright spots from laser-emitted light) and nonlabeled RBCs (halogen illumination source) recorded in the bottom plane ($z = 20\ \mu m$). (c) A confocal image used to track RBC motion. (d) A treated confocal image to visualize both RBCs and WBCs.
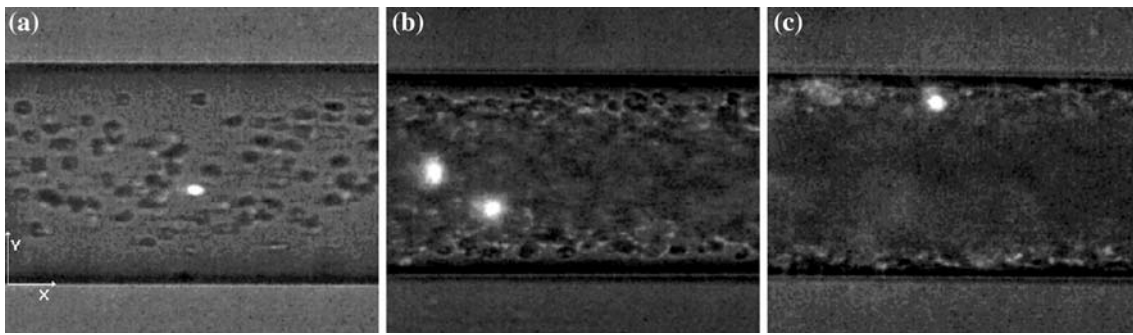
FIGURE 5. Halogen and confocal images in the middle plane with (a) 3% Hct, (b) 15% Hct, and (c) 35% Hct. The nonlabeled RBCs are observed as dark-gray rings, whereas labeled RBCs are observed as bright rings. It is possible to observe that the plasma layer tends to decrease with increasing Hct.

the plasma layer tends to decrease with an increasing Hct.

Motion of Individual RBCs

In vitro blood (20% Hct) was used to evaluate the ability of the proposed confocal system to investigate erythrocyte behavior in crowded environments (Re ~ 0.006). We were only able to measure cell–cell interactions at $z = 20$ μm, because of the formation of a plasma layer close to the wall. The microrheology phenomena studied were RBC–RBC and RBC–WBC hemodynamic interactions, as well as RBC orientation with and without interaction. Several representative examples are presented below. In this particular study, the hemodynamic interaction was quantified by the transversal displacement, $R_y(t)$, which is the y position normal to the direction of the flow in a time interval, t.

RBC–RBC Interactions in Flowing Blood

The individual interaction measurements shown in this study may help in further understanding the statistical values of the RBC dispersion coefficient obtained in a recent study performed by the current authors.[19] In this study, we showed the unique ability of the confocal system to obtain thin in-focus planes, allowing the measurement of the paths of two or more labeled RBCs interacting in the same focal plane. Although we were able to measure hundreds of individual RBC trajectories, measuring the interaction of two labeled RBCs was extremely complex. Two successful examples of RBC-RBC interaction within the plasma layer for a Re of ~0.006 are shown in Figs. 6 and 7. These examples show the effect on the trajectories of two interacting RBCs around the crowded boundary region of the plasma layer (Fig. 6) and adjacent to the microtube wall (Fig. 7).

Figure 6 shows typical trajectories of two RBC interactions around the crowded boundary region of the plasma layer, where the disturbance effect is increased by the collision of a neighboring RBC. Here, the transversal displacement (R_y) of both RBCs increased about 2–3 μm due to their collision ($t = 0.15$ s). For RBC 2, it is evident that the displacement continued to increase because of not only the current interaction but also other interactions with neighboring cells.

The trajectories of two RBCs interacting near the microtube wall are shown in Fig. 7. RBC 3 maintained a constant displacement along the wall (particularly for $t > 0.24$ s), whereas RBC 4 suffered an evident disturbance of its trajectory. These results suggest that the trajectories of RBCs rolling on the wall surface do not experience a strong hemodynamic effect from neighboring RBCs. Note that RBC 4 first undergoes a steep transversal displacement of about 3 μm, followed by a gradual decrease, probably as a result of collisions with the crowded suspension environment that exists adjacent to the plasma layer.

Figure 8 illustrates the instantaneous transversal positions of two RBCs (RBC 4 and RBC 2) that interacted continuously with neighboring RBCs at a 20% Hct. Transversal displacements of two noninteracting RBCs (RBCnoInt1 and RBCnoInt2) are also shown for a Hct of 3%. These results demonstrate that for the case of noninteracting RBCs, the magnitude of the transversal variability is always less than 1 μm, whereas RBCs flowing within a crowded environment experience greater variability in their trajectories, from ~2 up to 3 μm. Thus, the degree of convective dispersion is Hct dependent. These findings are consistent with those of our recent study on the determination of the RBC radial dispersion in a 100-μm microchannel at different Hcts.[19]

Orientation of RBCs in Flowing Blood

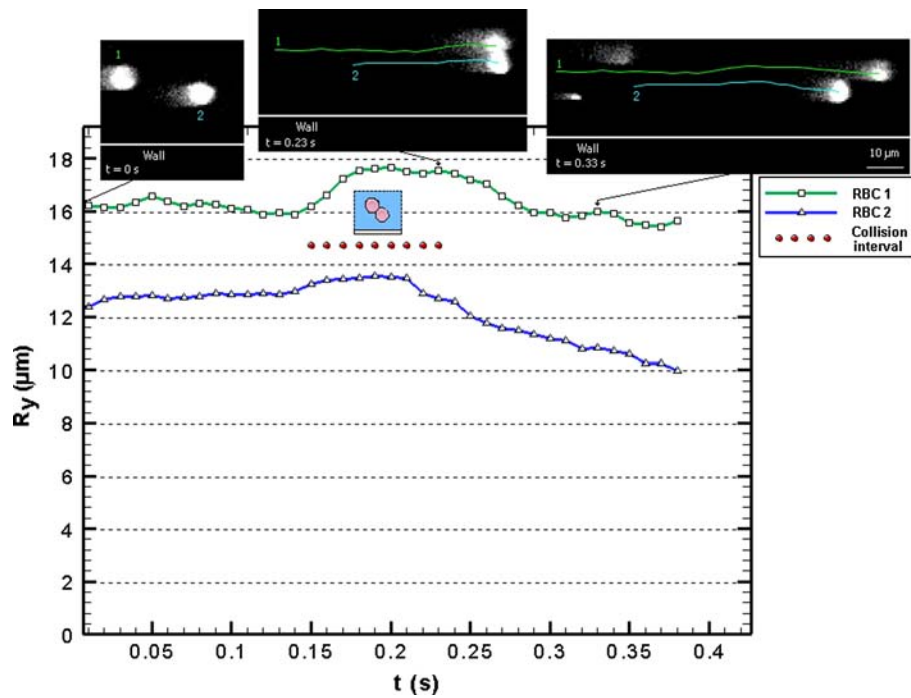The orientations of two RBCs with and without interaction were measured around the plasma layer

FIGURE 6. Two-RBC interactions at different times intervals (Re ~ 0.006). Instantaneous transversal displacement (R_y) of two-RBC interactions at 10 ms time intervals tracked in the bottom plane ($z = 20\ \mu m$) of a 100 μm diameter microchannel (see Electronic supplementary material 2).
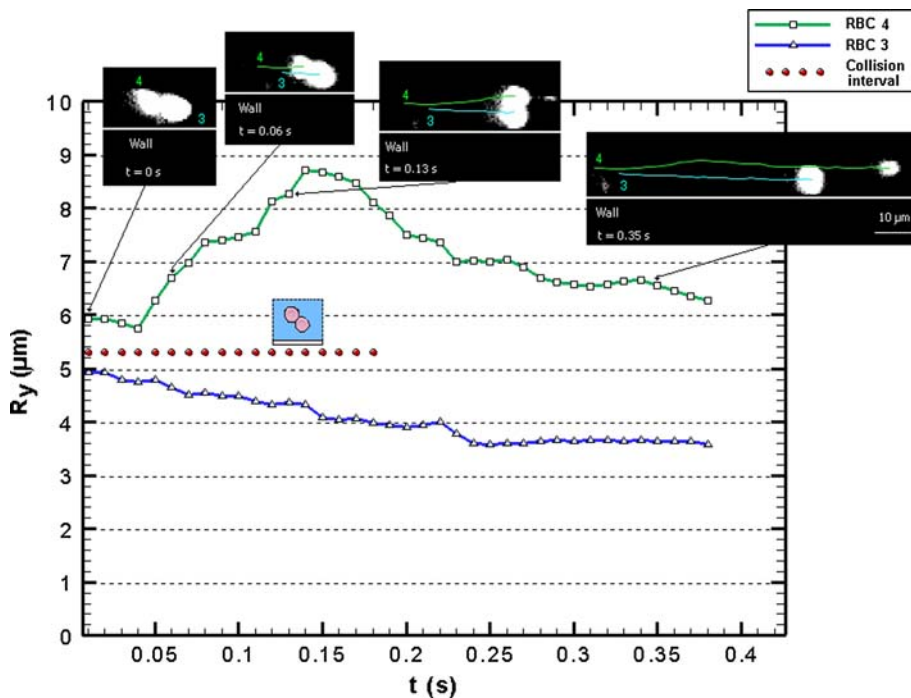

FIGURE 7. Two-RBC interactions near the wall (Re ~ 0.006). Instantaneous transversal displacement (R_y) of two-RBC interactions at 10 ms time intervals tracked in the bottom plane ($z = 20\ \mu m$) of a 100 μm diameter microchannel. RBC6 collides with a slower RBC rolling on the wall of the microchannel (see Electronic supplementary material 3).

in concentrated suspensions. By adjusting the image contrast, it was possible to measure both translational and rotational motion. The translational motions were measured at center of the RBC (based on the dark centroid criteria), whereas rotation was measured along the membrane (based on the
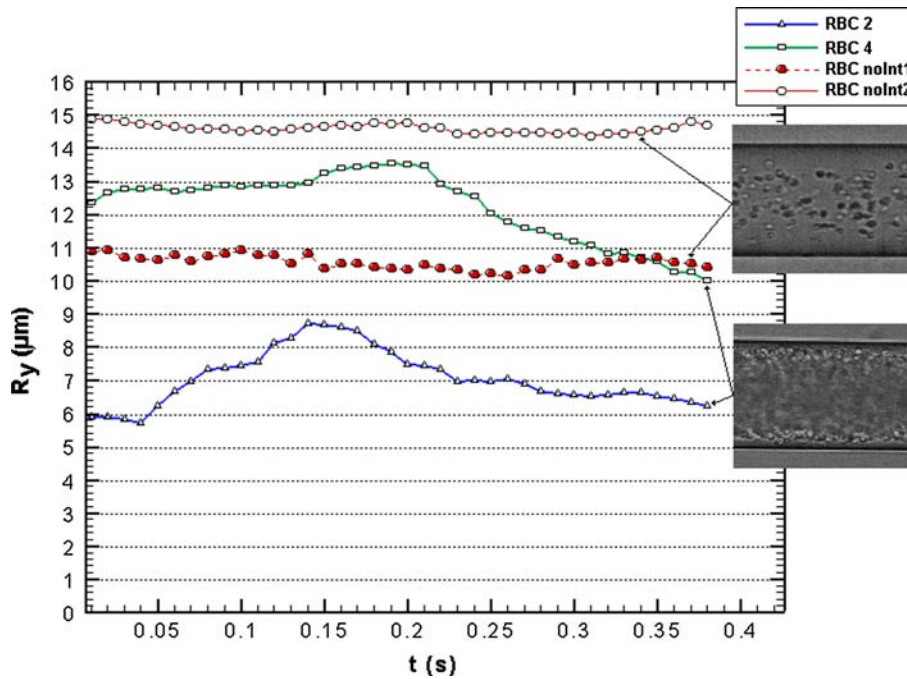
FIGURE 8. Comparison of the transversal displacement (R_y) between RBCs with interactions (20% Hct) and RBCs with no interactions at low Hct (3% Hct). RBCS traveling in dilute suspensions (3% Hct) tend to follow approximately linear trajectories, whereas at concentrated suspensions (20% Hct) RBCs suffer a variability in their trajectories of at least 1 μm from its original path.

bright centroid criteria), using MtrackJ[23] software (Fig. 9).

The brightness of fluorescently labeled RBCs depended strongly on their location within the microchannel. During the experiments, especially at locations close to the bottom wall (strongest incident light), we found that a small percentage of RBCs (less than 1% of the total cell volume) was partially labeled, creating small localized markers along the membrane. This phenomenon allowed us to determine the membrane motion of the partially labeled RBCs flowing near the microchannel wall ($z = 20 \ \mu$m).

The RBC without interaction was measured along the wall surface. This RBC did not interact with a neighboring RBC, allowing its translational transversal displacement to remain almost constant. Moreover, the RBC rotated as a biconcave disk in a clockwise direction with periodically varying angular motion. In contrast, RBCs interacting with neighboring cells demonstrated changes in both translational and rotational motions. These RBCs rotated in an erratic manner rather than in a regular and periodic way.

RBC–WBC Interactions in Flowing Blood

The hemodynamic interaction effects of WBCs on the motion of RBCs were also measured. Figure 10 shows the paths and corresponding transversal displacements of a RBC (RBC 5) interacting with the center upper part of a WBC (upper) and a RBC (RBC 6) interacting with the left side of the WBC (lower). Note that RBC 5 is located in the focal plane (high intensity) while the WBC is below the focal plane (lower intensity). Even though the WBC is not in the focal plane, the motion of RBCs is disturbed by its presence in the flow because of its size (typically twice that of a RBC) and geometry. Moreover, for both cases, the transversal displacement increased when a collision with a WBC occurred (Fig. 10). However, the displacement seemed to increase considerably when the RBC interacted with the side of a WBC. According to our observations, when RBCs interact around the center of a WBC, the displacement is larger in the z direction (depth of the microchannel). Although it was possible to visualize this three-dimensional displacement, our system currently does not allow quantification.

Dispersion of Labeled RBCs at Different Hcts

The random transversal motions of RBCs in directions normal to the flow can be analyzed using a dispersion coefficient (D_{yy})[14,16]:

$$D_{yy}(t) = \frac{1}{N} \sum_{i=1}^{N} \frac{\left\langle \left(R_{i,y}(t) - R_{i,y}(0) \right)^2 \right\rangle}{2t}, \quad (1)$$

where $\langle (R_{i,y}(t) - R_{i,y}(0))^2 \rangle$, t, and N are the mean square displacement, time interval, and number of
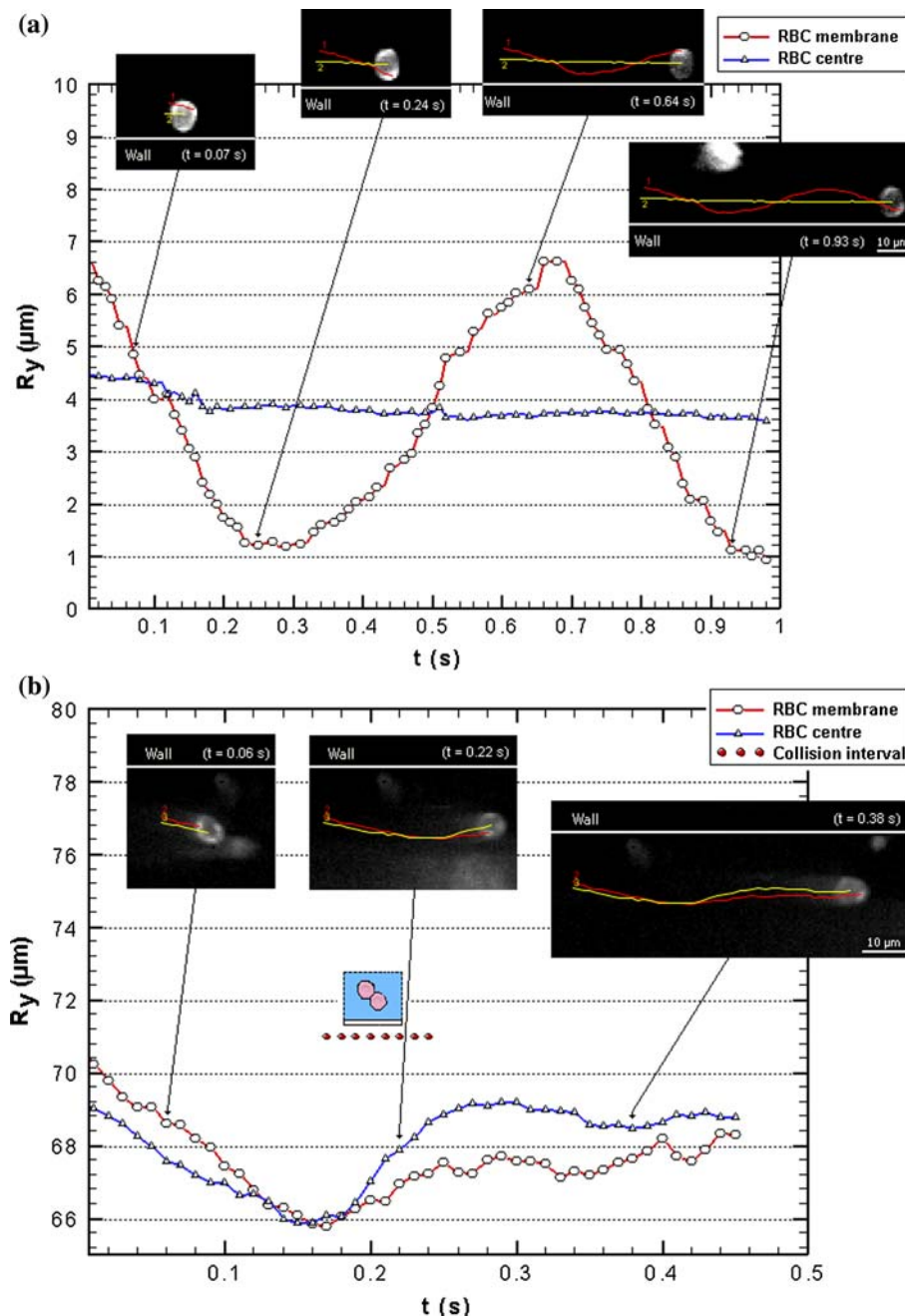
FIGURE 9. Instantaneous transversal displacement (R_y) of translational and rotational motion (Re ~ 0.006) at 10 ms time intervals tracked in the bottom plane ($z = 20~\mu$m) of a 100 μm diameter microchannel: (a) without interaction and (b) with interaction. The RBC rolling along the wall, which does not suffer any collision, tends to rotate in a regular and periodic way. In contrast, the RBC interacting with neighboring cells rotates in an erratic manner (see Electronic supplementary materials 4 and 5).

measured RBCs, respectively. Note that $R_{i,y}(t) - R_{i,y}(0)$ is the traversal displacement of individual RBC i in the xy confocal plane over some time interval, t.

The paths of multiple labeled RBCs were measured in the center plane and in focal planes located at 35 and 20 μm from the bottom of the microchannel (see Table 2). Figure 11 shows typical transversal displacements of RBCs in different focal planes for two different concentrations of RBCs (15 and 35% Hct). The corresponding RBC dispersion coefficients (D_{yy}) in three different focal planes for each Hct are shown in Fig. 12. The results show that D_{yy} tends to increase moving away from the microchannel axis, suggesting that the velocity gradients induced by the wall have a strong influence on the erratic transversal displacements shown in Fig. 12.
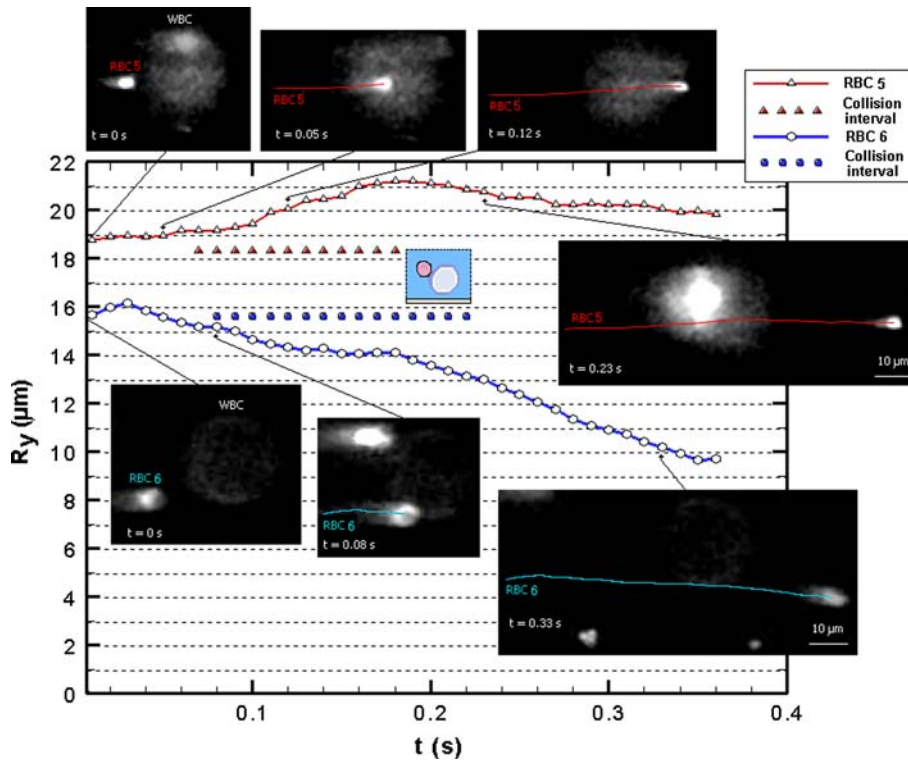
FIGURE 10. RBC–WBC interactions at 10 ms time intervals tracked in the bottom plane ($z = 20$ μm) of a 100 μm diameter microchannel (Re ~ 0.006). Instantaneous transversal displacement (R_y) of RBC 7 interacting with center upper part of a WBC (upper) and RBC 8 interacting with the left side of the WBC (lower). The RBCs paths are diverted due to collisions with WBCs; however, the lateral displacement seems to increase when the RBC interacts with the WBC lateral surface.

TABLE 2. Results of dispersion of labeled RBCs at different in-focus planes for 15 and 35% Hct.

Experiment	n^a	In-focus plane (z-axis, μm)	$D_{yy}^b \pm$ SD (cm^2/s)
RBC dispersion for 15% Hct	70	50	$3.0 \times 10^{-8} \pm 6.4 \times 10^{-9}$
	75	35	$4.2 \times 10^{-8} \pm 7.0 \times 10^{-9}$
	78	20	$4.2 \times 10^{-8} \pm 6.4 \times 10^{-9}$
RBC dispersion for 35% Hct	53	50	$4.3 \times 10^{-8} \pm 1.0 \times 10^{-8}$
	60	35	$5.3 \times 10^{-8} \pm 1.2 \times 10^{-8}$
	70	20	$6.5 \times 10^{-8} \pm 1.1 \times 10^{-8}$

[a]Number of labeled RBCs.
[b]Last value from the diagrams presented in Fig. 12.

DISCUSSION

Past research has identified temporal fluctuations in blood velocity profiles in microvessels. Most of these findings resulted from studies performed at macroscale and mesoscale levels. We believe that it is crucial to investigate the cause of this phenomenon at a cellular level. The data presented in this study demonstrate the ability of the confocal micro-PTV system to provide further insight into the complex flow behavior in microcirculation.

Blood Cell Interactions in Flowing Blood

Limitations in the current optical techniques that are used to investigate blood flow at a microscopic level have led to numerical studies on cell–cell interactions.[34,38] Nevertheless, experimental studies are essential to validate these numerical predictions. This study quantitatively and qualitatively characterized cell–cell hemodynamic interactions in flowing blood. The Re used in this study ranged from 0.0038 to 0.0058. At these low Re values, we did not observe obvious RBC aggregation. The use of Dx-40 might also have reduced the tendency toward aggregation.

The hemodynamic interactions of RBCs in concentrated suspensions depend on multiphysics hemodynamic parameters such as shear rate, plasma layer, and RBC deformability. We presented two typical RBC–RBC interactions in flowing blood. Generally, upon RBC interaction, transversal displacement tends to increase to a maximum peak. The cell rarely returns to its initial position, as interactions with other cells are likely. Two interesting phenomena happening within the plasma layer are presented. First, around the boundary of the plasma layer, where cells are crowded, migration toward the middle was inverted, owing to a
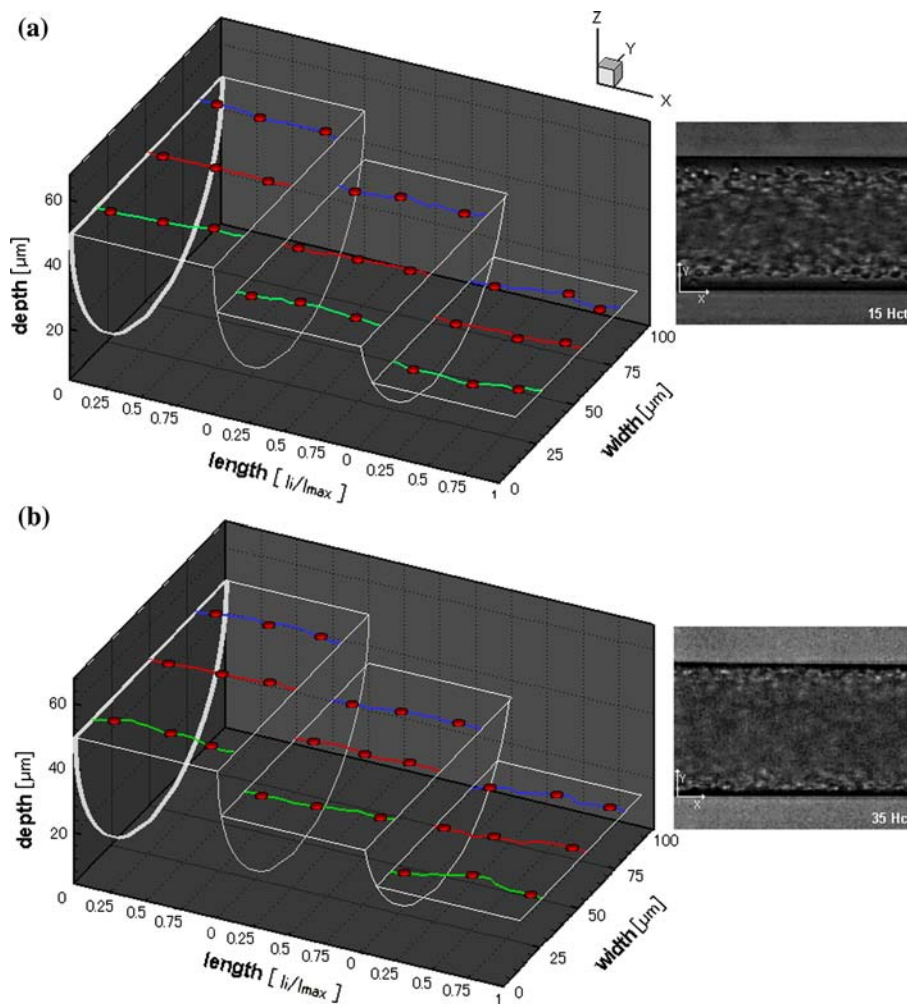
FIGURE 11. Instantaneous transversal displacement (R_y) of labeled RBCs at different in-focus planes for (a) 15% Hct and (b) 35% Hct (Re ~ 0.004). The RBC positions normal to the direction of the flow tend to increase moving away from the center plane of the microtube.

hemodynamic interaction with a RBC flowing in the crowded region (Fig. 6). Second, when a RBC was rolling on the surface, an interaction did not cause a significant increase in transversal displacement, indicating that the lubrication force between the RBC and the wall is greater than the hemodynamic force caused by the interaction (Fig. 7). Our results indicate that the plasma layer formed in microchannels is not completely cell free. Furthermore, these results suggest that a RBC flowing in the plasma layer is subjected to both axial and lateral migration, generating an undulating trajectory. Moreover, multibody collisions continuously divert RBC trajectories, inducing flow disturbances at a microscopic level. A statistical analysis based on a large number of collisions can be found in a recent study performed by the current authors.[19]

Generally, in dilute suspensions (Hct ~ 3%), RBCs tended to follow linear trajectories, as collisions with a neighboring cell were unlikely to occur. As the Hct increased, the RBCs began to experience transversal displacements of about 2% from the original path. At moderate Hcts (~20%) the RBCs flowing within the plasma layer tended to migrate toward the axis; however, this tendency was opposed in crowded region. Such resistance to crowding can enhance the fluctuations of the RBC trajectories, which eventually lead to an increase in wall collisions. This phenomenon may play an important role in the blood mass transport of cells and proteins to tissues and thrombi.

During our experiments, most of the WBCs were flowing near the bottom wall of the microtube. In this study, two representative RBC–WBC interactions were analyzed (Fig. 10). Note that some measurements of cell paths were performed with faint images (slightly out-of-focus cells). Our results suggest that the WBC hemodynamic effect on the trajectory of a RBC is dependent on the contact angle between the cells. For example, the transversal displacement of RBC 5
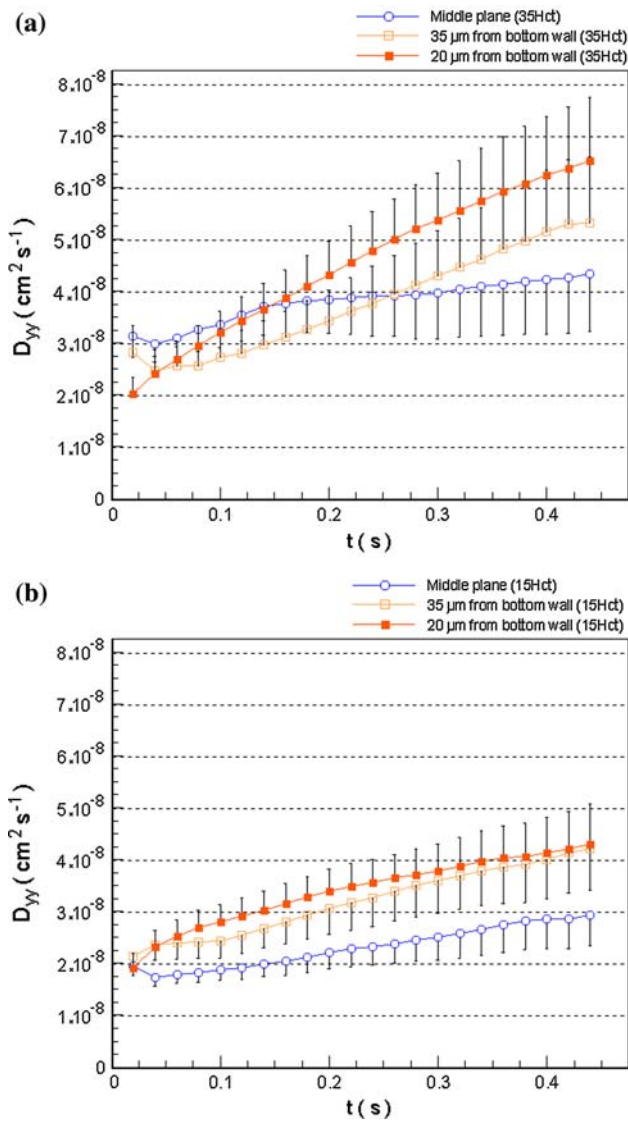
FIGURE 12. RBC transversal dispersion coefficients (D_{yy}) at different in-focus planes for (a) 15% Hct and (b) 35% Hct (Re ~ 0.004). D_{yy} tends to increase moving away from the center plane of the microtube. This phenomenon is a consequence of the combination of both radial and circumferential effects on the RBCs motions. Measured values are expressed as the mean ± standard deviation (95% confidence interval).

microchannel. At this region of high concentration, RBCs tended to get squeezed as they passed each other. Our study presents two remarkable examples of RBC orientation at low Re. The proposed technique provides information about both translational and rotational motions of a RBC with and without interaction. As shown in Fig. 9, interacting RBCs rotated erratically compared with cells rolling along the wall without interactions.

RBC Dispersion Coefficient

This study provides quantitative data on the transversal fluctuations of RBCs in different focal planes and at different Hcts. The transversal displacement and corresponding transversal dispersion coefficient tended to increase with decreasing z position (see Figs. 11 and 12). Thus, the RBCs that flowed near the wall had the highest transversal dispersion, which was a consequence of the combination of both radial and circumferential effects on the motions of RBCs traveling in the planes oriented out from the center axis. These results reinforce the evidence that both the local Hct and the velocity gradients induced by the wall play important roles in blood flow properties, which influence the resistance to blood flow in microvessels. Our detailed investigation of the complex effect of the Hct and microchannel diameter on the RBC radial dispersion coefficient can be found in our previous report.[19]

In previous studies, Goldsmith and colleagues[11–14] calculated radial dispersion coefficients using a fluid containing 39% ghost cells. Their values were slightly higher than the present results, especially near the wall.[19] This discrepancy might have been due to their use of RBCs without hemoglobin, which would affect RBC rheological properties. Moreover, the out-of-focus effect might have contributed to the measurements on RBCs located away from the focal plane of interest. A more detailed comparison can be found in Lima et al.[19]

Main Advantages and Limitations of the Proposed Confocal Micro-PTV

One of the main advantages of the proposed confocal micro-PTV system is the ability of the spinning disk confocal microscope (SDCM) to minimize background noise from the out-of-focus planes. Using a conventional microscope, the intensity of the RBCs in the out-of-focus planes does not change with the distance from the focal plane, resulting in an estimated depth of field[24] of up to four times the size of RBCs. In contrast, the brightness of the RBCs imaged with SDCM decreases dramatically near (1 μm from) the focal plane, providing greater contrast and true thin optical sections (2 μm in the current study). Hence,

increased by about 2 μm (Fig. 10) after it interacted with the upper center periphery of the WBC, while the transversal displacement of RBC 6 increased dramatically (>4 μm) after it interacted with the lateral surface of the WBC.

Orientation of RBCs in Flowing Blood

In our experiments (Re, 0.0071), we did not observe marked deformation, especially around the plasma layer. However, the degree of deformation seemed to increase as the RBCs migrated toward the center of the

SDCM systems provide accurate measurements of the paths of single RBCs or multi-RBC interactions flowing in the same focal plane, which is not possible using a conventional microscope.

One of the main limitations of using the SCDM is the low blood flow rate required to obtain accurate measurements. Our confocal system uses a CSU-22 scanning unit from Yokogawa, which allows us to obtain images at a rate of up to 2000 frames/s (0.5 ms between a pair of images). Although this temporal resolution can be achieved using dilute suspensions of RBCs, the images recorded using concentrated suspensions were too dark to be processed. Reasons for this limitation include not only the loss of incident illumination induced by the spinning disk pinholes but also the effect of the light scattered and absorbed by the RBCs. However, by decreasing the temporal resolution to 100 frames/s, it was possible to use a long exposure time (9.4 ms); this improved the image brightness, because the increase in the residence time of the labeled RBCs allowed the collection of sufficient photons for image formation. This approach was adequate for successfully measuring velocities up to 0.52 mm/s (Re ~ 0.007) in the center plane of the microchannel.[22] As the velocities in the microcirculation are typically between 0.2 and 10 mm/s,[4] our approach is suitable for studying microcirculation phenomena, especially in capillaries where the velocities are usually less than 1 mm/s.

The primary aim of this study was to develop a protocol for labeling RBCs with enough fluorescent probe to obtain images of sufficient quality for measurements using our confocal system. According to previous experiments,[14] healthy RBCs exhibit appreciable migration, whereas hardened RBCs do not. Recent experiments performed in a stenosed microchannel[9] have also shown clear differences in migration between healthy and hardened cells. These studies suggest that cell migration is strongly affected by cells deformability. Although in our experiments we always observed flows with a cell-free plasma layer on the wall and a cell-rich center core, we did not study the influence of the labeling procedure on the deformability of RBCs. In the near future, we expect to measure quantitatively the mechanical properties of individual labeled RBCs to determine the best experimental protocol, taking into account the compromise between the intensity of the emitted light versus the deformability of RBCs.

CONCLUSIONS

We applied a confocal micro-PTV system to measure the motion of individual RBCs through a 100-μm microchannel. The fluorescently labeled RBCs exhibited flow characteristics similar to those reported for flows in microvessels *in vivo*. This study characterized cell–cell hemodynamic interactions, RBC orientation, and RBC transversal dispersion at different depths in flowing blood with various hematocrit levels. In general, the results indicate that the plasma layer enhances collisions between neighboring RBCs, thereby influencing the motion and flow behavior of the cells. The results also provide evidence that multibody collisions promote fluctuations in the translational and rotational motions of RBCs. These findings confirm earlier observations and provide new insights into the complex behavior of RBCs flowing in a crowded environment. In summary, we have provided evidence that the proposed confocal micro-PTV system is a powerful technique for monitoring the paths of two or more blood cells interacting in the same focal plane. This method eliminates some difficulties with previous methods and provides additional details on the motions of RBCs that have not been obtainable with conventional methods.

ELECTRONIC SUPPLEMENTARY MATERIAL

The online version of this article (doi:10.1007/s10439-009-9732-z) contains supplementary material, which is available to authorized users.

REFERENCES

[1]Abramoff, M., P. Magelhaes, and S. Ram. Image processing with Image J. *Biophotonics Int*. 11:36–42, 2004.
[2]Baker, M., and H. Wayland. On-line volume flow rate and velocity profile measurement for blood in microvessels. *Microvasc. Res*. 7:131–143, 1974.
[3]Born, G., A. Melling, and J. Whitelaw. Laser Doppler microscope for blood velocity measurement. *Biorheology* 15:163–172, 1978.

[4]Caro, C., T. Pedley, R. Schroter, and W. Seed. The Mechanics of the Circulation. Oxford: Oxford University Press, 1978.

[5]Chien, S. Shear dependence of effective cell volume as a determinant of blood viscosity. *Science* 168:977–979, 1970.

[6]Conchello, J., and J. Lichtman. Optical sectioning microscopy. *Nat. Methods* 2:920–931, 2005.

[7]Fahraeus, R., and T. Lindqvist. The viscosity of the blood in narrow capillary tubes. *Am. J. Physiol.* 96:562–568, 1931.

[8]Fischer, T., M. Stohr-Lissen, and H. Schmid-Schonbein. The red cell as a fluid droplet: tank tread-like motion of the human erythrocyte membrane in shear flow. *Science* 202:894–896, 1978.

[9]Fujiwara, H., T. Ishikawa, R. Lima, N. Matsuki, Y. Imai, H. Kaji, M. Nishizawa, and T. Yamaguchi. Red blood cell motions in high-hematocrit blood flowing through a stenosed microchannel. *J. Biomech.* 42:838–843, 2009.

[10]Gaehtgens, P., H. Meiselman, and H. Wayland. Velocity profiles of human blood at normal and reduced hematocrit in glass tubes up to 130 μ diameter. *Microvasc. Res.* 2:13–23, 1970.

[11]Goldsmith, H. Red cell motions and wall interactions in tube flow. *Fed. Proc.* 30:1578–1588, 1971.

[12]Goldsmith, H. Deformation of human red cells in tube flow. *Biorheology* 7:235–242, 1971.

[13]Goldsmith, H., and J. Marlow. Flow behavior of erythrocytes. II. Particles motions in concentrated suspensions of ghost cells. *J. Colloid Interface Sci.* 71:383–407, 1979.

[14]Goldsmith, H., and V. Turitto. Rheological aspects of thrombosis and haemostasis: basic principles and applications. ICTH-Report-Subcommittee on Rheology of the International Committee on Thrombosis and Haemostasis. *Thromb. Haemost.* 55:415–435, 1986.

[15]Inoue, S., and T. Inoue. Direct-view high-speed confocal scanner: the CSU-10. In: Cell Biological Applications of Confocal Microscopy, edited by B. Matsumoto. San Diego: Academic Press, 2002, pp. 87–127.

[16]Ishikawa, T., and T. Pedley. Diffusion of swimming model micro-organisms in a semi-dilute suspensions. *J. Fluid Mech.* 588:437–462, 2007.

[17]Kinoshita, H., S. Kaneda, T. Fujii, and M. Oshima. Three-dimensional measurement and visualization of internal flow of a moving droplet using confocal micro-PIV. *Lab Chip* 7:338–346, 2007.

[18]Lima, R. Analysis of the blood flow behavior through microchannels by a confocal micro-PIV/PTV system. Ph.D. Thesis, Tohoku University, Japan, 2007.

[19]Lima, R., T. Ishikawa, Y. Imai, M. Takeda, S. Wada, and T. Yamaguchi. Radial dispersion of red blood cells in blood flowing through glass capillaries: role of hematocrit and geometry. *J. Biomech.* 41:2188–2196, 2008.

[20]Lima, R., S. Wada, M. Takeda, K. Tsubota, and T. Yamaguchi. *In vitro* confocal micro-PIV measurements of blood flow in a square microchannel: the effect of the haematocrit on instantaneous velocity profiles. *J. Biomech.* 40:2752–2757, 2007.

[21]Lima, R., S. Wada, S. Tanaka, M. Takeda, T. Ishikawa, K. Tsubota, Y. Imai, and T. Yamaguchi. *In vitro* blood flow in a rectangular PDMS microchannel: experimental observations using a confocal micro-PIV system. *Biomed. Microdevices* 10:153–167, 2008.

[22]Lima, R., S. Wada, K. Tsubota, and T. Yamaguchi. Confocal micro-PIV measurements of three dimensional profiles of cell suspension flow in a square microchannel. *Meas. Sci. Technol.* 17:797–808, 2006.

[23]Meijering, E., I. Smal, and G. Danuser. Tracking in molecular bioimaging. *IEEE Signal Process. Mag.* 23:46–53, 2006.

[24]Meinhart, C., S. Wereley, and H. Gray. Volume illumination for two-dimensional particle image velocimetry. *Meas. Sci. Technol.* 11:809–814, 2000.

[25]Meinhart, C., S. Wereley, and J. Santiago. PIV measurements of a microchannel flow. *Exp. Fluids* 27:414–419, 1999.

[26]Miyazaki, H., and T. Yamaguchi. Formation and destruction of primary thrombi under the influence of blood flow and von Willebrand factor analysed by a D. E. M. *Biorheology* 40:265–272, 2003.

[27]Nash, G., and H. Meiselman. Red cell and ghost viscoelasticity. Effects of hemoglobin concentration and in vivo aging. *Biophys. J.* 43:63–73, 1983.

[28]Park, J., C. Choi, and K. Kihm. Optically sliced micro-PIV using confocal laser scanning microscopy (CLSM). *Exp. Fluids* 37:105–119, 2004.

[29]Parthasarathi, A., S. Japee, and R. Pittman. Determination of red blood cell velocity by video shuttering and image analysis. *Ann. Biomed. Eng.* 27:313–325, 1999.

[30]Schmid-Schonbein, H., and R. Wells. Fluid drop-like transition of erythrocytes under shear. *Science* 165:288–291, 1969.

[31]Shiga, T., N. Maeda, and K. Kon. Erythrocyte rheology. *Crit. Rev. Oncol. Hematol.* 10:9–48, 1990.

[32]Sugii, Y., R. Okuda, K. Okamoto, and H. Madarame. Velocity measurement of both red blood cells and plasma of in vitro blood flow using high-speed micro PIV technique. *Meas. Sci. Technol.* 16:1126–1130, 2005.

[33]Tanaani, T., S. Otsuki, N. Tomosada, Y. Kosugi, M. Shimizu, and H. Ishida. High-speed 1-frame/ms scanning confocal microscope with a microlens and Nipkow disks. *Appl. Opt.* 41:4704–4708, 2002.

[34]Tsubota, K., S. Wada, and T. Yamaguchi. Particle method for computer simulation of red blood cell motion in blood flow. *Comput. Methods Programs Biomed.* 83:139–146, 2006.

[35]Uijttewaal, W., E. Nijhof, and R. Heethaar. Lateral migration of blood cells and microspheres in two-dimensional Poiseuille flow: a laser Doppler study. *J. Biomech.* 27:35–42, 1994.

[36]Vennemann, P., K. Kiger, R. Lindken, B. Groenendijk, S. Stekelenburg-de Vos, T. Hagen, N. Ursem, R. Poelmann, J. Westerweel, and B. Hierk. In vivo micro particle image velocimetry measurements of blood-plasma in the embryonic avian heart. *J. Biomech.* 39:1191–1200, 2006.

[37]Wootton, D., and D. Ku. Fluid mechanics of vascular systems, diseases, and thrombosis. *Annu. Rev. Biomed. Eng.* 1:299–329, 1999.

[38]Yamaguchi, T., T. Ishikawa, K. Tsubota, Y. Imai, M. Nakamura, and T. Fukui. Computational blood flow analysis—new trends and methods. *J. Biomech. Sci. Eng.* 1:29–50, 2006.